表1　生体肝提供者手術における術前・術中に要する画像診断

1. 腹部(肝)US
   ① 肝動脈，門脈，肝静脈肝走行の確認
   ② 波形・血流量・流入／出などの術前の確認
2. MD-CT
   ① Volimetry
   残肝容量　：ドナー切除後残肝容積率：＞35%
   移植肝容量：レシピエント・SLV：＞0.4(原則)
   ② 脈管構築：肝動脈，門脈，肝静脈
3. DIC-CT
   ① 胆管構築

走行の把握が重要である．そのために，術前に肝US (ultrasonography)，MD-CT (multidetector-CT)[1]と，可能な限りDIC-CTをドナー全例に施行し，その走行を術前に確認する．

1. 腹部(肝)US

術前にエコーを施行することにより，門脈，肝静脈の分枝などのスクリーニングを行う(図1a)．その際，温存し再建を施行しなければ，グラフトの肝鬱血をきたす可能性がある V5，V8 などについても，術前エコーでその場所を同定し，肝切離中の損傷を予防する．また，肝動脈(図1b)，門脈(図1c)，

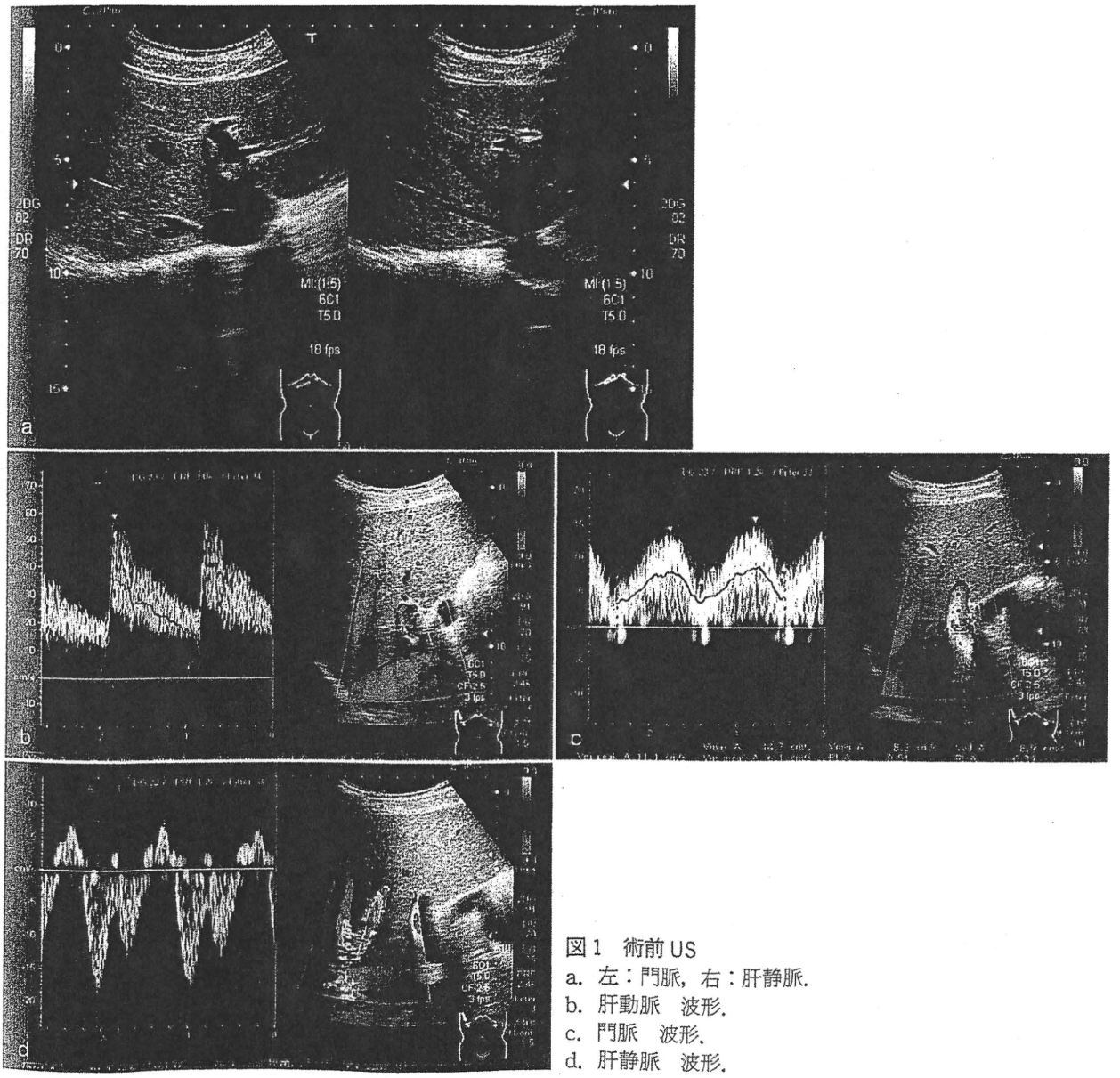

図1　術前US
a. 左：門脈，右：肝静脈．
b. 肝動脈　波形．
c. 門脈　波形．
d. 肝静脈　波形．

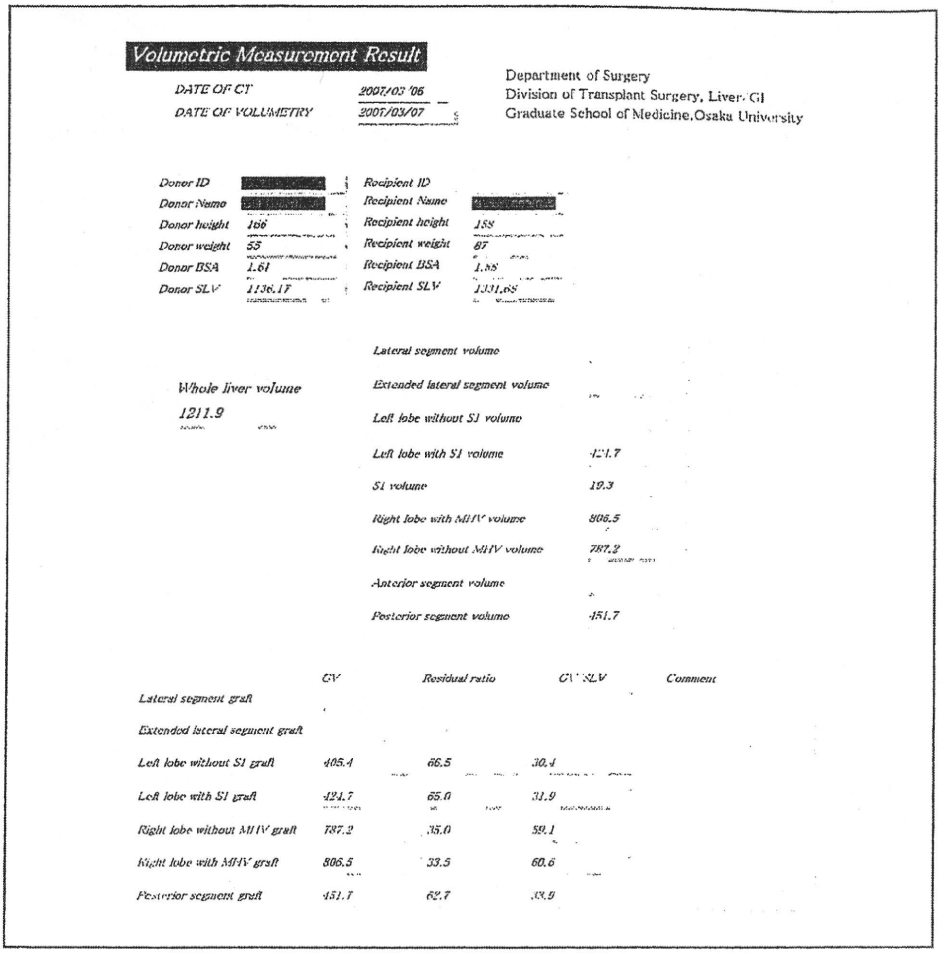

Volumetric Measurement Result

DATE OF CT 2007/03/06
DATE OF VOLUMETRY 2007/03/07

Department of Surgery
Division of Transplant Surgery, Liver, GI
Graduate School of Medicine, Osaka University

Donor ID		Recipient ID	
Donor Name		Recipient Name	
Donor height	166	Recipient height	158
Donor weight	55	Recipient weight	87
Donor BSA	1.61	Recipient BSA	1.88
Donor SLV	1136.17	Recipient SLV	1331.68

Whole liver volume
1211.9

Lateral segment volume	
Extended lateral segment volume	
Left lobe without S1 volume	
Left lobe with S1 volume	424.7
S1 volume	19.3
Right lobe with MHV volume	806.5
Right lobe without MHV volume	787.2
Anterior segment volume	
Posterior segment volume	451.7

	GV	Residual ratio	GV/SLV	Comment
Lateral segment graft				
Extended lateral segment graft				
Left lobe without S1 graft	405.4	66.5	30.4	
Left lobe with S1 graft	424.7	65.0	31.9	
Right lobe without MHV graft	787.2	35.0	59.1	
Right lobe with MHV graft	806.5	33.5	60.6	
Posterior segment graft	451.7	62.7	33.9	

図2 Volumetric Mesurementの結果の表

肝静脈(図1d)についての脈波形に加えて流量・流速などについても術前のコントロールとして確認しておく.

2. MD-CT

1) 移植肝容量

先述したように，生体部分肝移植手術における最優先事項は移植肝提供者の安全性である．そのために，肝切除容量[2]の過剰による術後肝不全については，100%回避する必要がある．筆者らは原則としてグラフト採取(肝切除術)後のドナー残肝容積率が35%以上になるように，また，移植肝がレシピエントの標準肝容量(レシンピエントの身長と体重より算定した予想肝容量)の40%以上になるように設定する．これはドナーに対して，過剰な肝切除を施行しないためには極めて重要である．

この術前の肝容積は術前のMD-CTを用いてvolumetryを施行し，算出する(図2)．また，最近では各sub-segmentごとの門脈支配領域や肝静脈還流領域などを3次元でvisualizeすることを可能にしたHepaVision and Interventional Plannner software tools(Melvis, Bremen, Germany)などのコンピュータソフトもあり，より詳細な情報を術前に得ることが可能になってきている．

2) 脈管構築

術前に肝動脈，門脈，肝静脈の分岐・走行を十分に把握するため，MD-CTを用いたコンピュータ画像処理を施行し，3次元構築を行い，詳細について把握する．

肝動脈(図3)：肝動脈走行には，解剖学的異常のある人が存在するため，動脈を切離する部位，吻合する脈管の部位，吻合する可能性のある動脈の本数などについて，十分に検討する．

門脈(図4)：門脈走行・分枝について確認する．特

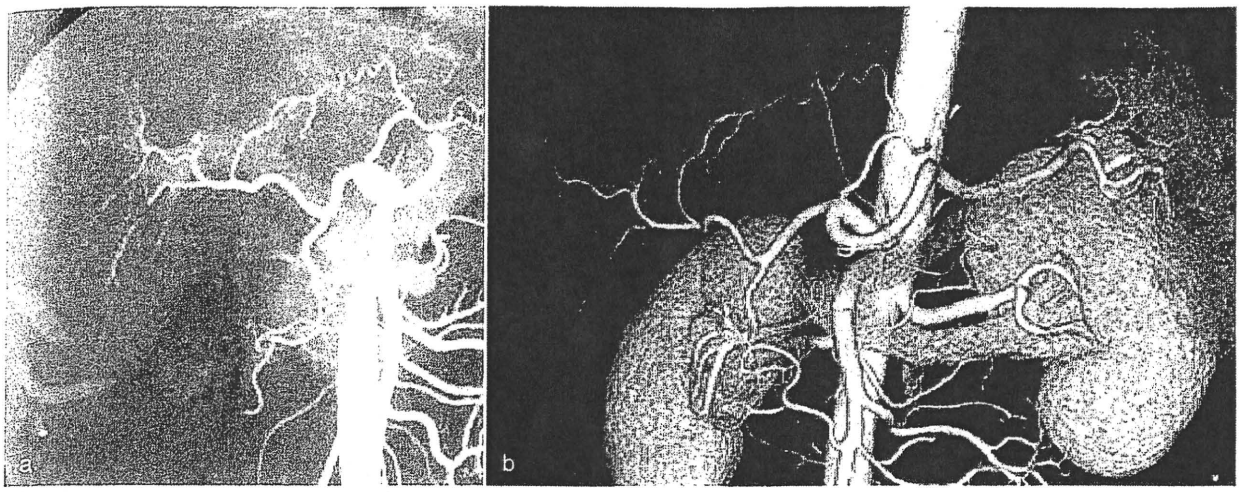

図3　MD-CT，肝動脈造影
a．動脈造影，b．3次元構築．

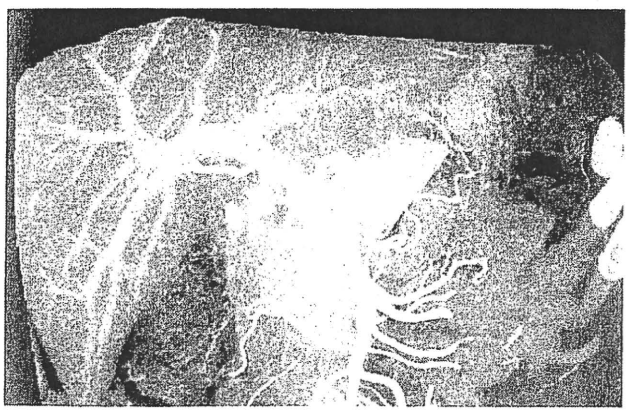

図4　MD-CT，門脈造影

に門脈の分枝については，採取するグラフトに種類を決定する重要な因子でもある．さらには，症例によっては門脈分枝異常と動脈走行の問題より，門脈吻合を要した症例[3]もある．図5は，54歳の女性のドナーの術前MD-CT(図5a)であるが，このドナーの肝切離の際に右肝動脈の後区域の枝が門脈本幹背側を走行していることがわかっていたため，グラフト採取の際に右肝動脈を温存するために門脈を切離し術中吻合再建した(図5b)．術前にこのようなanormalyが判明していたことより，術前に十分なインフォームド・コンセントが得られたとともに，術中の肝動脈損傷もなかった．

肝静脈：肝静脈の走行は，①術前の肝切離線の決定，②右下肝静脈の存在の有無についての診断，③右葉グラフト採取時の，肝静脈切離による鬱血領域出現の有無の推察，に有用である．図3は，MD-CTによる肝内静脈枝であるが，肝右葉グラフト採取・肝切離時に温存し，再建する可能性のある右下肝静脈(図6a)，V8(図6b)，V5(図6c)を示している．

3．DIC-CT

胆管の分岐・走行を把握するために，MD-CTに合わせてDIC-CTを施行し，同様に3次元構築を施行する(図7)．特に胆管の切離線の術前の把握に有用である．図8は中肝静脈付き左葉グラフト採取予定のドナーの術前DIC-CTであるが，後区域胆管が左肝内胆管より分枝しており，図8のAのところで胆管切離すると後区域胆管を離断することになるために，図8のBのところで切離する必要があった症例である．このDIC-CTの施行については，後述する術中胆道造影施行で，胆管の一次分枝の形態のみであればある程度代用可能であり，例えばレシピエントの術前疾患が劇症肝炎などのように手術の緊急性を要する場合には，省略せざるをえない場合もある．ただし図9に示したように，DIC-CTの施行により術中胆道造影では同定不可能なことが多い尾状葉胆管枝を術前に同定することが可能であり，尾状葉に分枝する胆管の不十分な処理がドナー肝切除術後の胆汁漏[4]の原因となることもあるため，その点での有用性は高い．

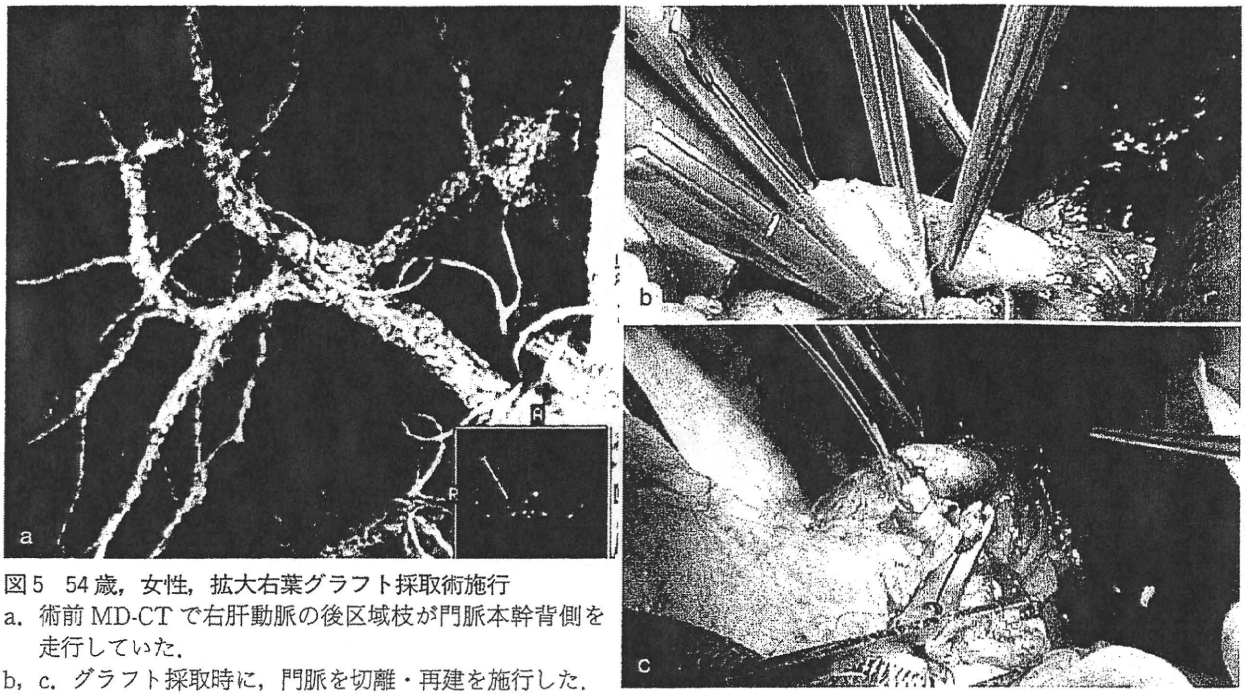

図5　54歳，女性，拡大右葉グラフト採取術施行
a．術前 MD-CT で右肝動脈の後区域枝が門脈本幹背側を走行していた．
b，c．グラフト採取時に，門脈を切離・再建を施行した．

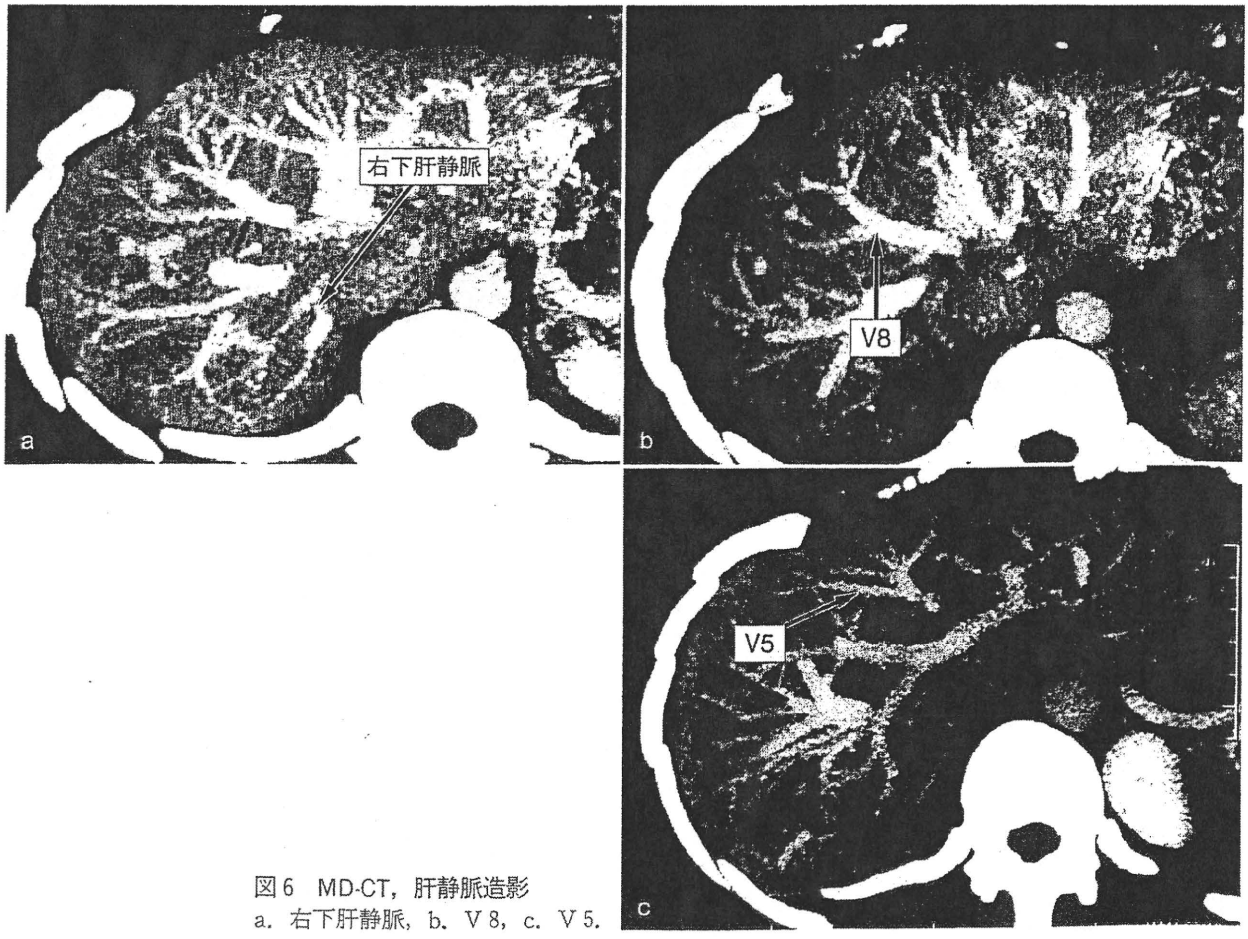

図6　MD-CT，肝静脈造影
a．右下肝静脈，b．V 8，c．V 5．

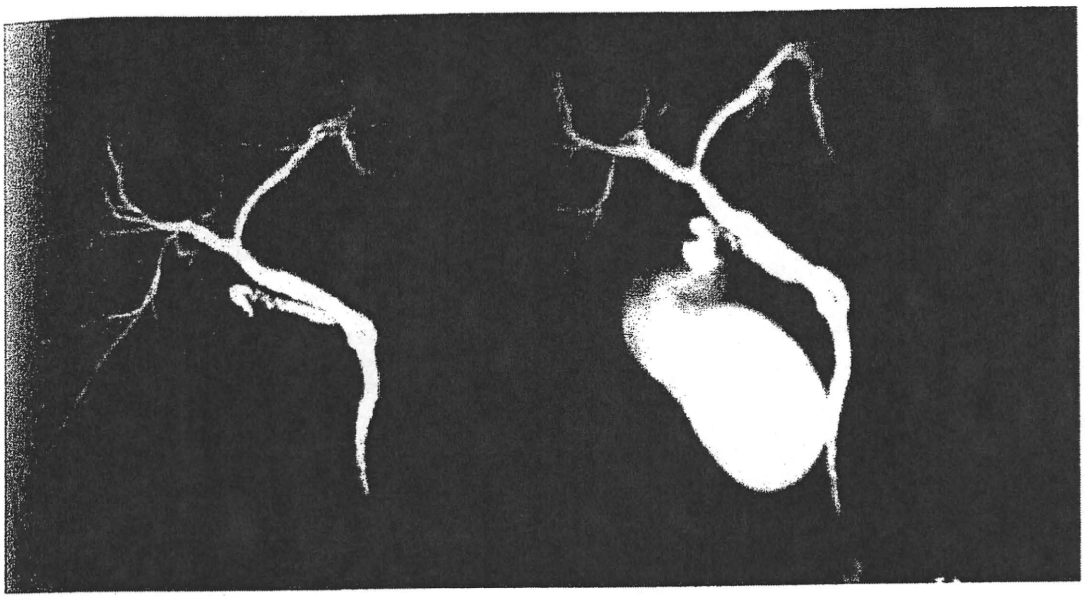

図7　DIC-CT，3次元構築

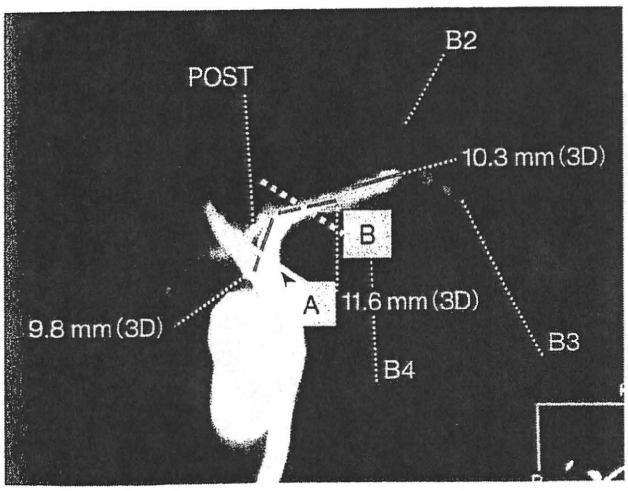

図8　DIC-CT，左葉グラフト症例

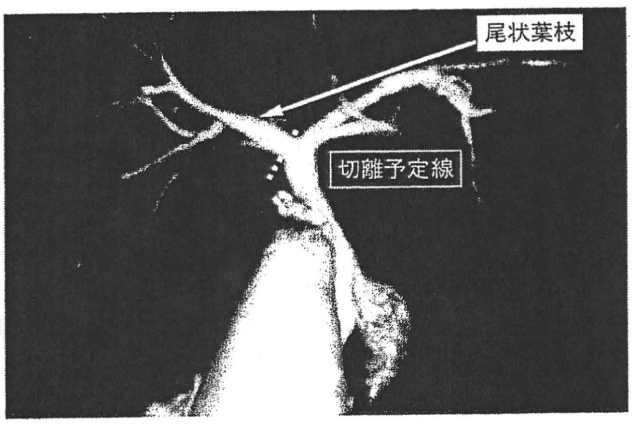

図9　DIC-CT，右葉グラフト症例
尾状葉胆管枝が描出されている．

おわりに

以上のように，生体部分肝移植手術における移植肝提供者手術においては，術前の画像診断が，その手術を安全かつ円滑に施行するためには極めて有用である．

ちなみに，現在までに大阪大学消化器外科においては，生体部分肝移植手術におけるドナー手術を142例施行してきたが，全例において，術中(非自己)輸血を必要とすることもなく，安全にドナー肝摘出(肝切除)術を施行している．

◎文献

1) 大坪毅人，高崎　健，山本雅一．生体肝移植ドナー肝における3DCTの有用性．今日の移植 2002；15：373-375
2) Yamanaka N, Okamoto E, Kawamura E, et al. Dynamics of normal and injured human liver regeneration after hepatectomy as assessed on the basis of computed tomography and liver function. Hepatology 1993；18：79-85
3) Marubashi S, Dono K, Nagano H, et al. Portal venous reconstruction in a living liver donor with an anomalous hepatic arterial and portal venous anatomy. J

Gastrointest Surg 2005 ; 9 : 365-368
4) Umeshita K, Fujiwara K, Kiyosawa K, et al. For the Japanese Liver Transplantation Society : operative morbidity of liver donors in Japan. Lancet 2003 ; 362 : 687-690

ORIGINAL ARTICLE

Suppression of *Hath1* Gene Expression Directly Regulated by Hes1 Via Notch Signaling Is Associated with Goblet Cell Depletion in Ulcerative Colitis

Xiu Zheng, MD, Kiichiro Tsuchiya, MD, PhD, Ryuichi Okamoto, MD, PhD, Michiko Iwasaki, MD, PhD, Yoshihito Kano, MD, Naoya Sakamoto, MD, PhD, Tetsuya Nakamura, MD, PhD, and Mamoru Watanabe, MD, PhD

Background: The transcription factor *Atoh1/Hath1* plays crucial roles in the differentiation program of human intestinal epithelium cells (IECs). Although previous studies have indicated that the Notch signal suppresses the differentiation program of IEC, the mechanism by which it does so remains unknown. This study shows that the undifferentiated state is maintained by the suppression of the *Hath1* gene in human intestine.

Methods: To assess the effect of Notch signaling, doxycycline-induced expression of Notch intracellular domain (NICD) and Hes1 cells were generated in LS174T. *Hath1* gene expression was analyzed by quantitative reverse-transcription polymerase chain reaction (RT-PCR). Hath1 promoter region targeted by HES1 was determined by both reporter analysis and ChIP assay. Expression of Hath1 protein in ulcerative colitis (UC) was examined by immunohistochemistry.

Results: Hath1 mRNA expression was increased by Notch signal inhibition. However, Hath1 expression was suppressed by ectopic HES1 expression alone even under Notch signal inhibition. Suppression of the *Hath1* gene by Hes1, which binds to the 5′ promoter region of Hath1, resulted in suppression of the phenotypic gene expression for goblet cells. In UC, the cooperation of aberrant expression of HES1 and the disappearance of caudal type homeobox 2 (CDX2) caused Hath1 suppression, resulting in goblet cell depletion.

Conclusions: The present study suggests that Hes1 is essential for *Hath1* gene suppression via Notch signaling. Moreover, the suppression of Hath1 is associated with goblet cell depletion in UC. Understanding the regulation of goblet cell depletion may lead to the development of new therapy for UC.

(Inflamm Bowel Dis 2011;000:000–000)

Key Words: ulcerative colitis, Hath1, Hes1, Notch signaling

The gut epithelium undergoes continual renewal throughout adult life, maintaining the proper architecture and function of the intestinal crypts. This process involves highly coordinated regulation of the induction of cellular differentiation and the cessation of proliferation, and vice versa.[1–3] Many studies of the regulation of intestinal differentiation have shown that cellular formation of the villi in small and large intestine is affected by various intracellular signaling pathways such as Notch, Wnt, and BMP.[4–7] Moreover, recent studies have also shown that dysregulation of the differentiation system for prompt intestinal epithelial cell formation induces the pathology of such intestinal diseases as colon cancer, Crohn's disease and ulcerative colitis (UC).[8] Then it was suggested that crucial genes for the differentiation of intestinal epithelium cells (IECs) become corrupt by aberrant cell signaling on the pathogenesis of intestinal diseases.

One of the most important genes for cell formation is a basic helix-loop-helix (bHLH) transcription factor, *Atoh1*, and its human homolog, *Hath1*, which is essential for the differentiation toward secretory lineages in small and large intestine.[9] Using a ubiquitin proteasomal system, we demonstrated that regulation of Hath1 protein in colon carcinogenesis is regulated by glycogen synthase kinase 3β (GSK3β) via Wnt signaling. Moreover, Hath1 and β-catenin protein are reciprocally regulated by GSK3β in Wnt signaling for the coordination between cell differentiation and

Additional Supporting Information may be found in the online version of this article.

Received for publication November 9, 2010; Accepted November 15, 2010.

From the Department of Gastroenterology and Hepatology, Graduate School, Tokyo Medical and Dental University, Tokyo, Japan.

Supported in part by grants-in-aid for Scientific Research 19209027, 21590803, 21790651, and 21790653, from the Japanese Ministry of Education, Culture, Sports, Science and Technology; JFE (Japanese Foundation for Research and Promotion of Endoscopy); Japan Foundation for Applied Enzymology; Intractable Diseases, the Health and Labor Sciences Research Grants from the Japanese Ministry of Health, Labor and Welfare.

The first two authors contributed equally to this work.

Reprints: Mamoru Watanabe, MD, PhD, MD, PhD, Professor and Chairman, Department of Gastroenterology and Hepatology, Graduate School, Tokyo Medical and Dental University, 1-5-45 Yushima, Bunkyo-ku, Tokyo 113-8519, Japan (e-mail: mamoru.gast@tmd.ac.jp)

DOI 10.1002/ibd.21611

Published online 00 Month 2011 in Wiley Online Library (wileyonlinelibrary.com).

proliferation. These findings together indicate that the deletion of adenomatous polyposis coli (APC) in colon carcinogenesis causes Hath1 protein degradation by switching the target of GSK3β from β-catenin to Hath1, resulting in maintenance of the undifferentiated state.[10] The dysregulation of prompt differentiation of IEC thus causes major intestinal diseases, and elucidation of the roles of various cell-signaling pathways in intestine is therefore important in understanding the pathogenesis of intestinal diseases.

We have also recently reported aberrant expression of Notch intracellular domain (NICD) in lesions showing goblet cell depletion in UC patients.[8] Moreover, forced expression of NICD caused the suppression of phenotypic genes for goblet cells in human intestinal epithelial cells. It has also been reported that forced expression of NICD in murine intestinal epithelial cells caused the depletion of goblet cells with the decrease of Atoh1 expression.[5] Thus, it is likely that *Atoh1* gene expression is regulated by Notch signaling, leading to subsequent control of intestinal epithelial cell lineage decision of the crypt cells.

The regulation of Hath1, however, is less well understood in human intestine. In previous reports, regulation of *Atoh1* gene expression was assessed using the mouse or chicken promoter region,[11,12] but the critical domains of the mouse and chicken sequences are not completely conserved in the Hath1 promoter region and enhancer region. To date, the regulation of *Hath1* gene expression has not been assessed using the human sequence. In particular, it remains unknown how *Hath1* gene expression is suppressed by Notch signaling in the intestine. It also remains unknown whether goblet cell depletion in UC is affected by Hath1 expression in intestinal epithelial cells.

In this study we demonstrated that Hes1 expression via Notch signaling is enough to suppress the *Hath1* gene by directly binding to the 5′ promoter region of Hath1. In UC, the cooperation of Hes1 and caudal type homeobox 2 (CDX2) caused the suppression of Hath1, resulting in the goblet cell depletion.

MATERIALS AND METHODS

Cell Culture

Human colon carcinoma-derived LS174T cells were maintained in minimum essential medium supplemented with 10% fetal bovine serum and 1% penicillin-streptomycin, 4 mM L-glutamine. Except where indicated otherwise, cells were seeded at a density of 5×10^5 cells/mL in each experiment. Cell cultures and transfections of plasmid DNA were performed as previously described.[6] A cell line expressing Notch1 intracellular domain (NICD), Hes1, HeyL (Tet-On NICD, Tet-On Hes1, Tet-On HeyL cells) under the control of doxycycline (DOX, 100 ng/mL, ClonTech, Palo Alto, CA) was generated as previously described.[8] The cell lines were supplemented with Blastcidin (7.5 μg/mL, Invitrogen, La Jolla, CA) and Zeocin (750 μg/mL, Invitrogen) for maintenance. The inhibition of Notch signaling was achieved by the addition of LY411,575 (1 μM).

Quantitative Real-time Polymerase Chain Reaction (PCR)

Total RNA was isolated with Trizol reagent (Invitrogen) according to the manufacturer's instructions. Aliquots of 1 μg of total RNA were used for cDNA synthesis in 20 μL of reaction volume. One microliter of cDNA was amplified with Cyber Green in a 20-μL reaction as previously described.[6] The primer sequences in this study are summarized in Supporting Information Table S1.

Plasmids

5′ Hath1 reporter plasmid was generated by cloning a 1031-bp sequence 5′ of the human *Hath1* gene (corresponding to −1,029 to +2 of the promoter region) into a pGL4 basic vector (Promega, Madison, WI). Hath1 reporter plasmid containing the 3′ region was generated by cloning a 4811-bp sequence 3′ of the human *Hath1* gene (corresponding to +1401 to +6211 of the Hath1 genome) into the 5′ Hath1 reporter plasmid. Internal deletion mutants of the 5′ Hath1 reporter plasmid in which three Hes1 binding sites CACGCG (−305 to −300, −269 to −264, −159 to −154) were replaced with GTCGAC were constructed by PCR-mediated mutagenesis.[13] Doxycycline-dependent expression of NICD was achieved by cloning the gene encoding the intracellular portion of the mouse Notch1 into the pcDNA4/TO/myc-his vector (Invitrogen).[8] Doxycycline-dependent expression of Hes1 was achieved by cloning the gene encoding rat Hes1 into the pcDNA4/TO/myc-his vector (Invitrogen). Doxycycline-dependent expression of HeyL was achieved by cloning the gene encoding human HeyL into the pcDNA4/TO/myc-his vector (Invitrogen). All constructs were confirmed by DNA sequencing.

Luciferase Assays

LS174T cell seeded in a 6-well plate culture dish were transfected with 4 μg of reporter plasmid along with 10 ng of pRL-tk plasmid (Promega). Cells were harvested 36 hours after transfection, lysed by three cycles of freezing and thawing, and the luciferase activities in each sample as indicated by arbitrary unit were normalized against Renilla luciferase activities as previously described.[10]

Chromatin Immunoprecipitation Assay

A chromatin immunoprecipitation (ChIP) assay was performed essentially as previously described with some modifications.[6] LS174T/Hes1 cells were seeded onto a 150-mm dish, then stimulated with DOX or left untreated for 12 hours. Immunoprecipitation was performed overnight at 4°C with 10 μg of an anti-Hes1 (a kind gift from Dr. T. Sudo), normal mouse immunoglobulin G (sc-2025, Santa Cruz Biotechnology, Santa Cruz, CA), or an anti-histone H3 antibody (Abcam,

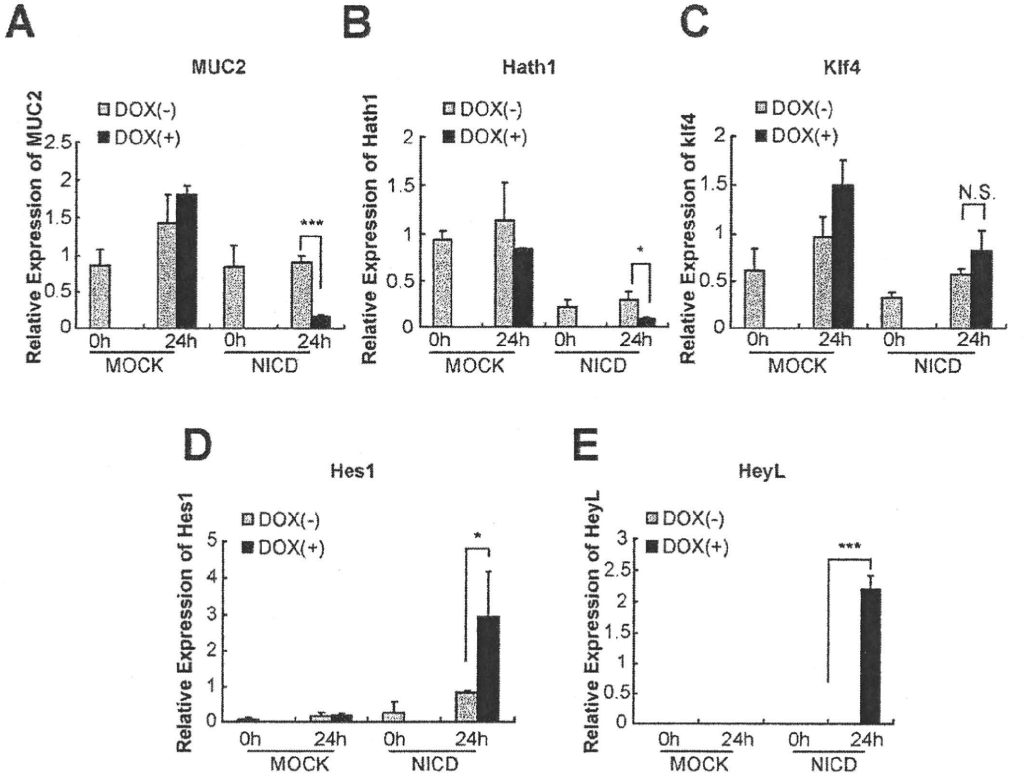

FIGURE 1. Gene alternation in LS174T cells by the expression of NICD. NICD is induced by DOX using the Tet-on system to mimic the acceleration of the Notch signal in LS174T cells. NICD expression by DOX decreased the expression of MUC2 (A) and Hath1 (B) genes. Klf4 gene expression was not affected (C). NICD also induced expression of Hes family genes such as Hes1 (D) and HeyL (E). (*$P < 0.05$, ***$P < 0.001$, $n = 3$).

Cambridge, MA). The genomic DNA fragments in the immunoprecipitated samples were analyzed by PCR using primers indicating the positions on the genomic DNA relative to the translation start site (Supporting Information Table 1). The same amounts of DNA samples were analyzed by conventional PCR in parallel with the following parameters: denaturation at 94°C for 15 seconds, annealing at 60°C for 30 seconds, and extension at 68°C for 60 seconds for 45 cycles. The products were resolved by agarose gel electrophoresis, stained with ethidium bromide, and visualized using an ImageQuant TL system (GE Healthcare, Milwaukee, WI).[6] The primer sequences in this study are summarized in Supporting Information Table S1.

Human Intestinal Tissue Specimens

Human tissue specimens were obtained from patients who underwent endoscopic examination or surgery at Yokohama Municipal General Hospital or Tokyo Medical and Dental University Hospital. Normal colonic mucosa was obtained from patients with colorectal cancer who underwent colectomy. Each of three patients with UC and colon cancer were examined. Written informed consent was obtained from each patient and the study was approved by the Ethics Committee of both Yokohama Municipal General Hospital and Tokyo Medical and Dental University.

Immunohistochemistry

Hath1 antibody (1:5000) was originally generated as previously described. Hes1 antibody (1:10,000) was the same as in the ChIP assay. Fresh frozen tissue was used after microwave treatment (500W, 10 minutes) in 10 mM citrate buffer for Hath1 and Hes1. The standard ABC method (Vectastain; Vector Laboratories, Burlingame, CA) was used, and staining was developed by addition of diaminobenzidine (Vector Laboratories).

Statistical Analyses

Quantitative real-time PCR analyses were statistically analyzed with Student's *t*-test. *P* less than 0.05 was considered statistically significant.

RESULTS

Notch Signaling Suppresses *Hath1* Gene Expression But Not Kuppel-like Factor 4 (Klf4) Gene in Human IECs

Expression of Atoh1 seems to be regulated at its transcriptional level, as forced expression of NICD in murine IECs causes the decrease of Atoh1 mRNA expression and subsequent depletion of goblet cells in vivo.[5] We therefore assessed the effect of the Notch signal on the expression of

Hath1 in a human intestinal epithelial cell line, LS174T cells. NICD is induced by DOX using a Tet-on system to mimic the acceleration of the Notch signal. NICD expression showed not only the decrease of Mucin2 (MUC2) expression but also a significant decrease of *Hath1* gene expression (Fig. 1A,B). We also assessed Klf4 gene expression by NICD expression because Klf4 is also essential to goblet cell differentiation.[14] Klf4 gene expression, however, was not affected by forced NICD expression (Fig. 1C), since it is suggested that the suppression of goblet cell phenotypic gene expression by Notch signaling is independent of Klf4 expression.

To assess how Notch signaling suppresses the gene expression of Hath1, we selected the Hes1 and HeyL genes as possible suppressors, based on previous identification of the Hes family genes induced by NICD in LS174T cells using a microarray system.[8] We confirmed that the gene expression of Hes1 and HeyL was markedly induced by NICD expression (Fig. 1D,E).

Hes1 But Not HeyL Suppresses *Hath1* Gene Expression in Human IECs, Resulting in the Decrease of MUC2 Gene Expression

To assess which genes suppress the *Hath1* gene expression, we generated cells (LS174T Tet-on Hes1 cells and LS174T Tet-on HeyL cells) in which either Hes1 or HeyL is induced by DOX using the Tet-on system, respectively. Forced expression of Hes1 alone showed a significant decrease of MUC2 gene expression following the decrease of *Hath1* gene expression (Fig. 2A,B). In contrast, HeyL induction alone did not change the expression of either MUC2 (Fig. 2A) or Hath1 genes (Fig. 2B). Moreover, neither Hes1 nor HeyL induction affected Klf4 gene expression (Fig. 2C). These results are compatible with previous reports that the depletion of Hes1 in a mouse model upregulated Atoh1 mRNA expression in intestinal epithelial cells, resulting in the hyperplasia of the goblet cells.[15] Conversely, the finding that Klf4 was not affected by the Notch signaling differs from previous reports.[16]

Hes1 Expression Alone Is a Sufficient Condition for the Repression of the Phenotypic Gene Expression of Goblet Cells by Notch Signaling

To further analyze the functional role of Notch signaling in the differentiation of IECs, we next asked whether Hes1 expression alone is enough to compensate for the suppression of *Hath1* gene expression in Notch signaling. To inhibit the Notch signaling, LS174T Tet-on Hes1 cells were treated with gamma-secretase inhibitor (GSI), which prevents the separation of NICD from the Notch receptor. Notch signal inhibition by GSI treatment alone showed a significant decrease of Hes1 gene expression (Fig. 3A), in contrast to marked induction of MUC2

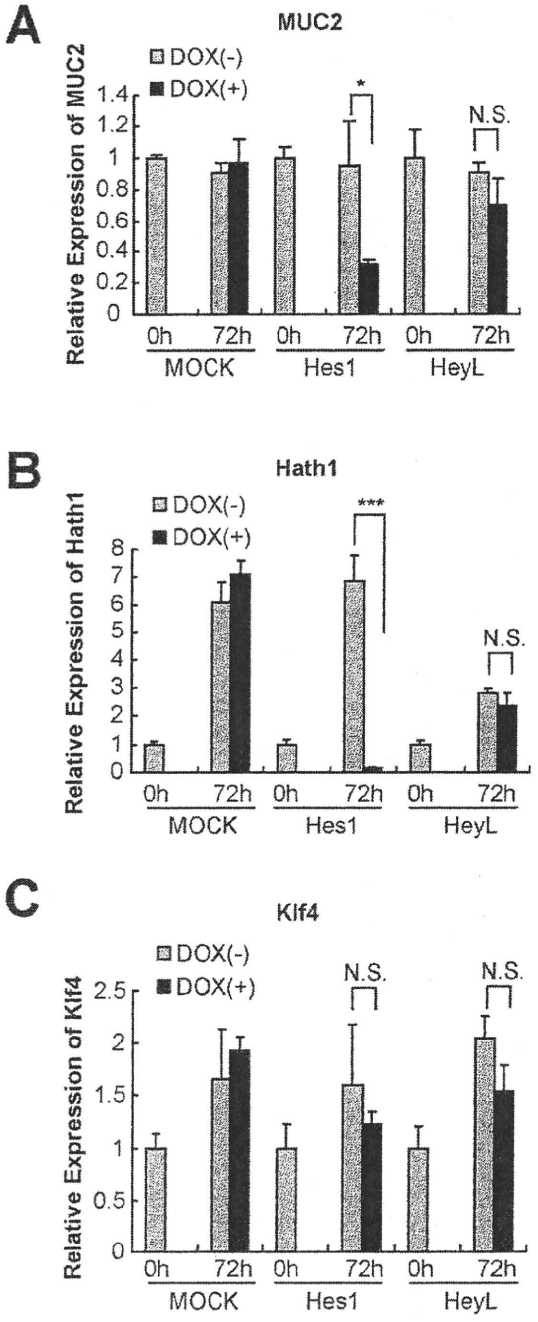

FIGURE 2. Gene alternation in LS174T cells by the expression of either Hes1 or HeyL. (A) Hes1 or HeyL was induced by DOX in LS174T Tet-on Hes1 cells or LS174T Tet-on HeyL cells, respectively. Hes1 induction significantly decreased MUC2 gene expression. (B) Hes1 induction resulted in a significant decrease of Hath1. (C) Neither Hes1 nor HeyL induction affected Klf4 gene expression. (*$P < 0.05$, ***$P < 0.001$, $n = 3$).

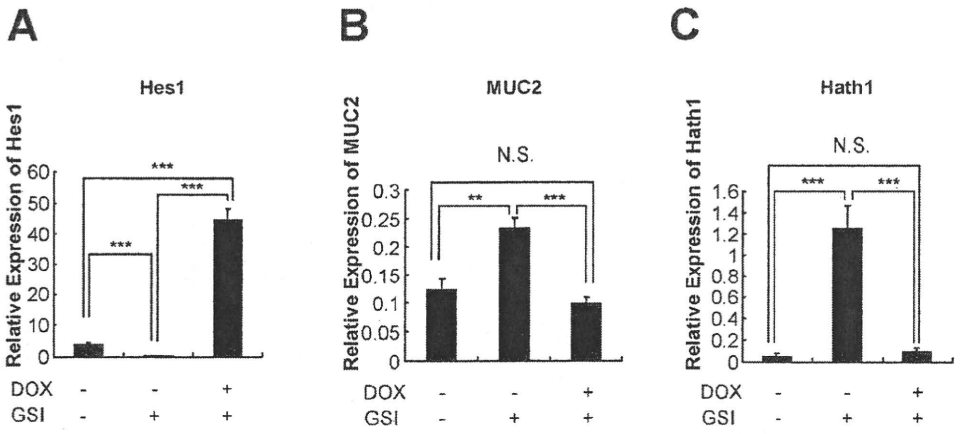

FIGURE 3. Hes1 expression is enough to suppress intestinal cell differentiation by Notch signaling. (A) LS174T Tet-on Hes1 cells were treated with GSI, which prevents the separation of NICD from the Notch receptor. GSI treatment alone significantly decreased Hes1 gene expression. Hes1 was induced by DOX in addition to GSI. (B) GSI markedly induced MUC2 gene expression. Hes1 induction by DOX in GSI-treated cells restored MUC2 gene expression to the level in untreated cells. (C) GSI markedly induced *Hath1* gene expression. Hes1 induction by DOX in GSI-treated cells restored *Hath1* gene expression to the level in untreated cells. (**$P < 0.01$, ***$P < 0.001$, $n = 3$).

gene expression (Fig. 3B) following the induction of the *Hath1* gene (Fig. 3C). Interestingly, the Hes1 gene was expressed by DOX when Notch signaling was inhibited by GSI (Fig. 3A), while Hath1 expression was restored to the level in untreated cells (Fig. 3C). Moreover, MUC2 gene expression was also decreased by Hes1 expression alone (Fig. 3B).

These results indicate that Hes1 might be a mainstream of Notch signaling to suppress the phenotypic gene expression of goblet cells in human intestine.

Previous results raised the question of whether Hath1 is essential for expression of the MUC2 gene by Notch signaling inhibition. To assess the importance of the *Hath1* gene for MUC2 expression, the effect of silencing the *Hath1* gene using siRNA system was examined in LS174T cells in the Notch signaling-inhibited state. *Hath1* gene silencing resulted in cancellation of the *Hath1* gene expression induced by GSI treatment and restoration of MUC2 expression to the level in untreated cells (Supporting Information Fig. 1).

These results together suggest that Notch signaling affects the gene expression of Hath1 but not Klf4 to decide the fate of IECs.

HES1 Suppresses the Transcriptional Activity of Hath1 Via the 5′ Promoter Region

It has been reported that expression of Math1, the mouse homolog of Atoh1, was suppressed by ZIC1 or HIC1 via its 3′ region.[12,17] However, it has never been shown how Hes1 suppresses the transcriptional activity of Hath1 via Notch signaling. To assess the regulation of Hath1 transcriptional activity, we constructed a reporter plasmid containing the 1000-bp upstream 5′ region of Hath1. Hath1 reporter plasmid was transfected into LS174T Tet-on Hes1 cells or LS174T cells transfected with a mock plasmid. Hes1 induction by DOX showed a significant decrease of the transcriptional activity on Hath1, whereas the mock plasmid did not change its transcriptional activity (Fig. 4A). We then found three regions that matched the consensus sequence for binding Hes1, the Class C site,[18] in the 1000-bp upstream region of Hath1. We therefore constructed a reporter plasmid in which all regions of the Hes1 binding site in the 1000-bp upstream region of Hath1 were deleted. As expected, reporter activity of the deletion mutant construct was not suppressed by Hes1 expression. We next constructed mutants in which one of the binding sites of Hes1 in the 1000-bp upstream region of Hath1 was deleted. Interestingly, only the mutant construct lacking the second region of the Hes1 binding site was not affected by Hes1, indicating that Hes1 might directly suppress the Hath1 transcriptional activity to bind to the second region of the Hes1 binding site (Fig. 4A).

In chicken and mouse models, Atoh1 expression is regulated only by the 3′ region of Atoh1 that contains both the enhancer region and the repressor region.[12,19] We also found a homologous sequence of the enhancer region in the 3′ region of Hath1, and a Hes1 binding site in this enhancer region of Hath1. We therefore constructed a Hath1 reporter plasmid containing the 3′ region of Hath1 behind the luciferase sequence. As before, Hes1 suppressed Hath1 transcriptional activity. Moreover, deletion mutants of the Hes1 binding site in the 5′ region of Hath1 were also unaffected by Hes1 expression, indicating that the Hes1 binding site of the 3′ region might not affect Hath1 suppression by Hes1 (Fig. 4B).

HES1 Binds Directly to the 5′ Promoter Region of Hath1

To confirm the binding of Hes1 to Hath1 promoter region, we performed a ChIP assay. The region immunoprecipitated by Hes1 antibody was amplified only in the 5′ region

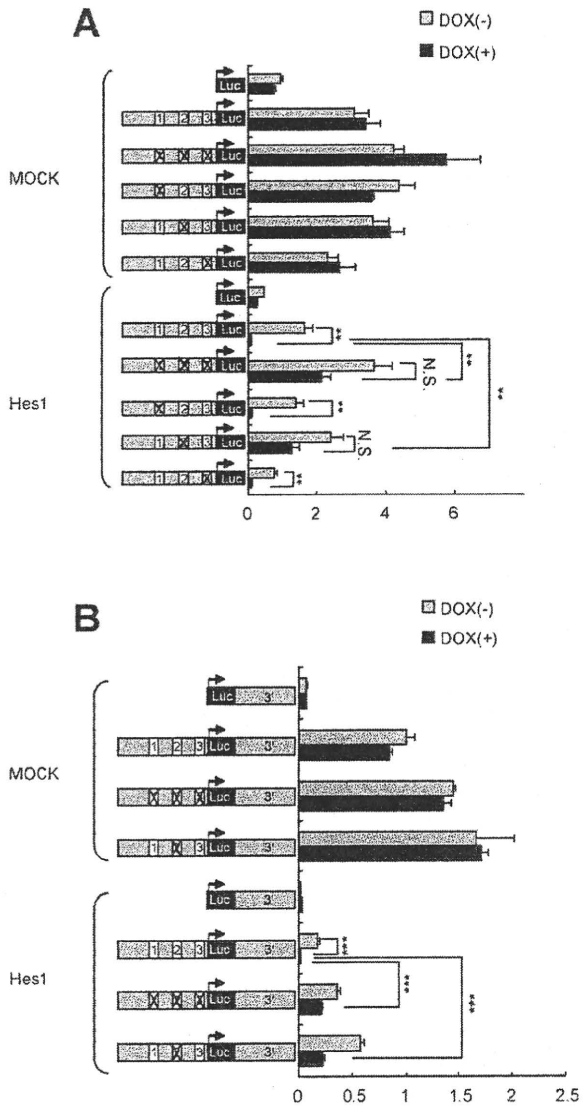

FIGURE 4. Hes1 regulates the transcriptional activity of Hath1 via 5′ promoter region. (A) 5′ Hath1 reporter plasmid containing the 1000-bp upstream region of Hath1 was transfected into LS174T Tet-on Hes1 cells and LS174T cells transfected with a mock plasmid. The induction of Hes1 by DOX significantly decreased the transcriptional activity on Hath1, whereas the transcriptional activity of the mock plasmid did not change. Three regions that matched the consensus sequence for binding Hes1, the Class C site, in the 1000-bp upstream region of Hath1 are indicated as square numbers. Reporter activity of a mutant with all regions of the Hes1 binding site deleted was not suppressed by Hes1 expression. A mutant construct in which only the second region of the Hes1 binding site was deleted was also unaffected by Hes1. (B) Hath1 reporter plasmid containing the 3′ enhancer region of Hath1 behind the luciferase sequence was inserted into 5′ Hath1 reporter plasmid. Hes1 also suppressed Hath1 transcriptional activity enhanced by 3′ enhancer region. The deletion mutants of the Hes1 binding site in the 5′ region of Hath1 were also unaffected by Hes1 expression (B). (**$P < 0.01$, ***$P < 0.001$, $n = 3$).

including the Hes1 binding sites but not 3′ region of the Hes1 binding sites (Fig. 5B), supporting the idea that Hes1 binds directly to the 5′region of Hath1 to suppress the transcriptional activity in IEC.

Hes1 Does Not Completely Block the Transcriptional Activity of Hath1 Promoted by CDX2

To clarify the balance between the enhancer and the repressor in Hath1 transcriptional activity, we next assessed whether CDX2, which promotes *Atoh1* gene transcription in mice, is affected by Notch signaling on Hath1 transcription. Treatment with GSI showed slight induction of CDX2 in LS174T cells (Fig. 6A). Moreover, HES1 expression did not affect the expression of CDX2 (Fig. 6B), suggesting that the expression of CDX2 may be independent of Notch signaling. To assess the effect of CDX2 on Hath1 transcription regulated by HES1, a reporter assay of Hath1 was performed. Although CDX2 did not promote Hath1 transcription via the 5′ promoter region of Hath1 (Fig. 6C), CDX2 cotransfected with the reporter plasmid containing the 3′ enhancer region of Hath1 showed significant increase of transcriptional activity of Hath1 (Fig. 6D). Interestingly, the transcriptional activity of Hath1 promoted by CDX2 was not suppressed by Hes1 induction in LS174T tet-HES1 cells. These results suggest that Hes1 at the 5′ region of Hath1 could not completely abrogate the transcriptional activity of Hath1 promoted via the 3′ enhancer region by CDX2, and *Hath1* gene expression might be regulated by the balance between HES1 and CDX2.

Hath1 Protein Expression Is Decreased in the Goblet Cell Depletion of UC

We finally assessed whether Hath1 is decreased in colon mucosa with goblet cell depletion in line with the former results in vitro. In normal colonic mucosa, Hath1 and CDX2 were expressed in almost all IECs. In contrast, Hes1 was expressed in IECs situated in the lower half of the villi (Fig. 7). In UC patients, both Hath1 and CDX2 disappeared, while Hes1-positive cells were extended at the top of the villi (Fig. 7), indicating that the suppression of Hath1 in goblet cell depletion might be caused by both the disappearance of CDX2 and the extension of Hes1-positive cells.

DISCUSSION

This study reveals for the first time that Hes1 directly suppresses *Hath1* gene expression via the Notch signal, indicating that downregulation of Hath1 is associated with goblet cell depletion in human UC in combination with the disappearance of CDX2. Previous reports have suggested that Notch signaling suppressed the phenotypic gene expression of goblet cells by suppressing *Atoh1* gene expression,[5] although it remains unknown how Notch signaling suppresses

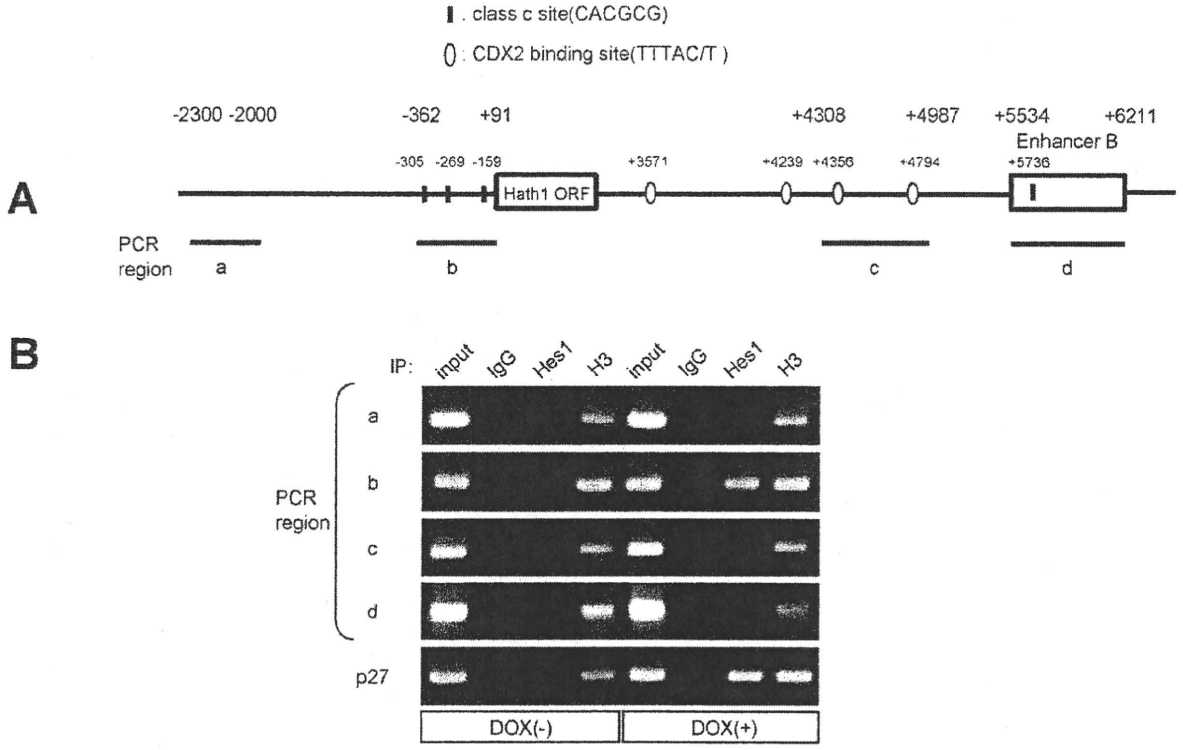

FIGURE 5. Hes1 binds to 5′ Hath1 promoter region. (A) Schematic presentation of Hath1 genome. (B) ChIP assay was performed using LS174T Tet-on Hes1 cells with or without DOX treatment for 24 hours. Each region indicated by a letter in (A) was amplified from the immunoprecipitant by each antibody. The amplification of p27 from the immunoprecipitant by Hes1 antibody was confirmed to be the known region of the Hes1 binding site. Only the 5′ region including the Hes1 binding sites of Hath1 (region b) was amplified from the immunoprecipitant by Hes1 antibody under the induction of Hes1 expression by DOX.

Hathl gene expression. We first found that Hes1, but not HeyL, was necessary and sufficient for the suppression of *Hathl* gene expression by Notch signaling in IEC. Canonical Notch signaling leads to transcriptional activation of Hes family and Hey family genes such as Hes1, Hes5, Hes7, Hey1, Hey2, and HeyL by binding NICD to RBP-Jk.[20] Hes and Hey family genes play important roles in the differentiation of various tissues,[21,22] but it has not been clarified how the function of each gene is assigned via Notch signaling. While we found that all Hes and Hey family genes were upregulated by NICD expression in intestinal cells, we also noticed that Hes1 and HeyL were exorbitantly expressed by NICD than other Hes and Hey family genes (data not shown), suggesting that the functional assignment of Notch signaling is regulated by the quantity of each Hes and Hey family gene expressed. HeyL has been identified as one of the target genes of Notch3 receptor, because HeyL is expressed in smooth muscle cells of the digestive tract and the vasculature following Notch3 expression in later stages of development.[23] In this study, we could not identify the function of HeyL in goblet cell differentiation; rather, its function is expected to be assessed in future study of the effect of Notch signaling on IEC.

On the other hand, we found that Hes1 is critical for the differentiation into goblet cells via Notch signaling, since the binding of HES1 to the Hath1 5′ promoter region silences *Hathl* gene expression. Although the 3′ region of Atoh1 has been characterized as the enhancer and repressor region to regulate *Hathl* gene expression by CDX2, Zic1, and Hic1, the function of the 5′ region of Atoh1 has not been clarified. This study revealed that the 5′ region of Hath1 is necessary not only for basic transcription but also for the regulation by HES1 via Notch signaling to presumably suppress the transcriptional activity of the basic transcription factors. It has been reported that Hes1 binds not only to the N-box sequence but also to class C sites to suppress the expression of genes such as $P27^{kip118}$ and achaete-scute homolog-1,[24] through which it plays a central role in cell proliferation and differentiation, respectively. In this study we identified a class C site at position −289 of the 5′ region of Hath1, playing a crucial role in the regulation of *Hathl* gene expression by the Notch signal. We therefore suspected that Hes1 might completely shut out the transcriptional activity via the

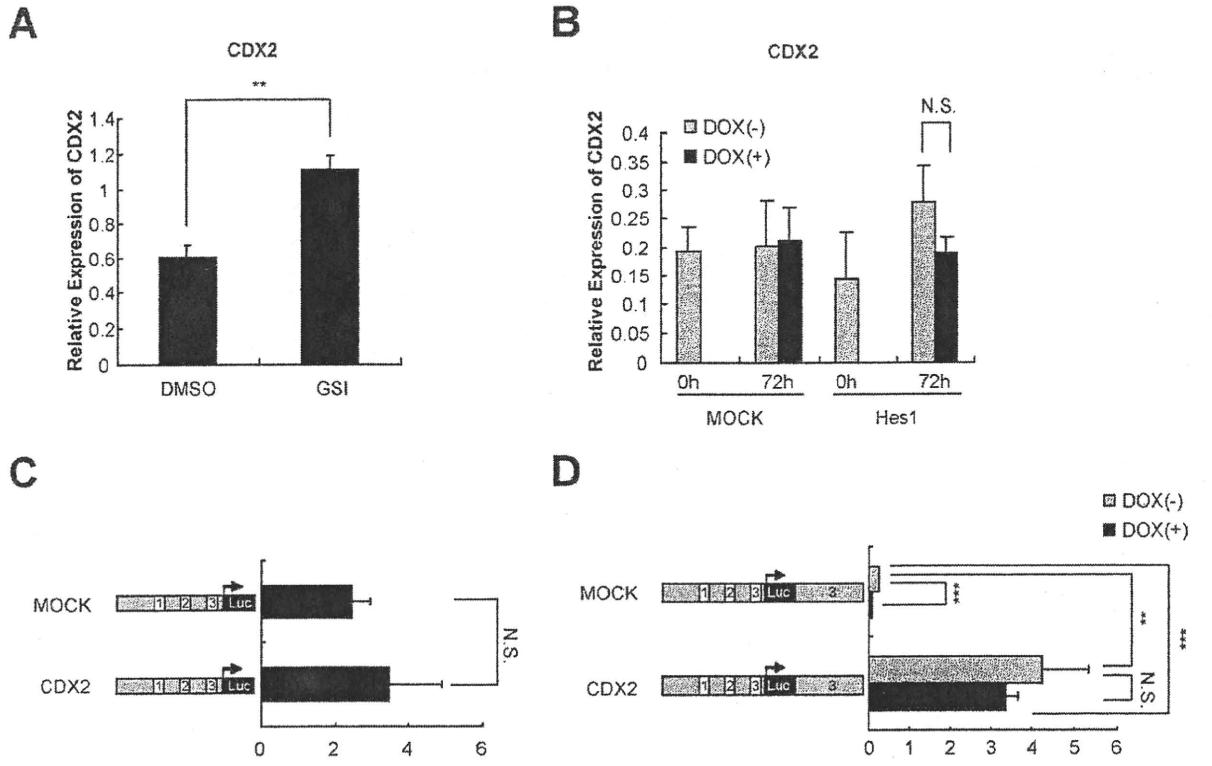

FIGURE 6. CDX2 enhances the transcriptional activity of Hath1 independently of Notch signaling. (A) *CDX2* gene expression was analyzed by treatment of LS174T cells with GSI for 72 hours. CDX2 was slightly upregulated by Notch signal inhibition. (B) *CDX2* gene expression was analyzed by the Hes1 expression induced by DOX in LS174T Tet-on Hes1 cells. *CDX2* gene expression was not affected by Hes1 expression. (C) Transcriptional activity of Hath1 via the 5′ region by CDX2 was assessed in LS174T cells for 72 hours after transfection of both the *CDX2* gene and 5′ Hath1 reporter plasmid. CDX2 did not affect the transcriptional activity via the 5′ promoter region of Hath1. (D) HES1 did not suppress the transcriptional activity via the 3′ region of Hath1 by forced expression of CDX2. The transcriptional activity of Hath1 was assessed for 72 hours after transfection of both the *CDX2* gene and 3′ Hath1 reporter plasmid with or without DOX in LS174T Tet-on HES1 cells. (**$P < 0.01$, ***$P < 0.001$, $n = 3$).

3′ enhancer region, but that forced expression of CDX2 could induce the transcriptional activity of Hath1 even with Hes1 expression. Moreover, the expression of CDX2 was not affected by Notch signaling, suggesting that CDX2 and HES1 independently regulate *Hath1* gene expression. Thus, regulation by Hes1 via Notch signaling is not sufficient to suppress the gene transcription of *Hath1*, indicating that the transcriptional activity of Hath1 is regulated by the balance between CDX2 and HES1 expression.

Importantly, the present study also indicated that Hath1 is essential to regulate goblet cell formation in UC. Although the expression of Hath1 in inflamed mucosa of UC has been reported,[25] the correlation between goblet cell content and Hath1 expression in UC has not been elucidated. We confirmed that Hath1 was expressed in inflamed mucosa with conserved goblet cell formation in UC (data not shown), since goblet cell content might correlate with Hath1 expression in UC. In Atoh1-deficient mice, secretory lineages of IEC including goblet cells are completely lost,[9,26] indicating that Hath1 might have the function of not only mucus production but also differentiation toward goblet cells in human intestine.

Moreover, this study suggested that goblet cell depletion in UC caused by the disappearance of Hath1 required not only HES1 expression but also CDX2 suppression of IEC. CDX2 has been reported to be downregulated in UC mucosa,[27] but it remains unknown how CDX2 expression is suppressed by colonic inflammation even though CDX2 is upregulated by inflammation in the esophagus and stomach.[28,29] One previous report indicated that CDX2 expression is suppressed by hypoxia inducible factor 1 (HIF1).[30] Another report found that HIF1 is overexpressed in UC mucosa,[31] suggesting that HIF1 might suppress CDX2 expression in UC. Whatever the case, the regulation of CDX2 expression of IEC should be assessed to clarify the mechanism of goblet cell depletion in UC.

In conclusion, we have revealed for the first time that Hes1 is sufficient to suppress *Hath1* gene transcription via the Notch signal, but insufficient to suppress *Hath1* gene transcription by CDX2. The cooperation between Hes1 and

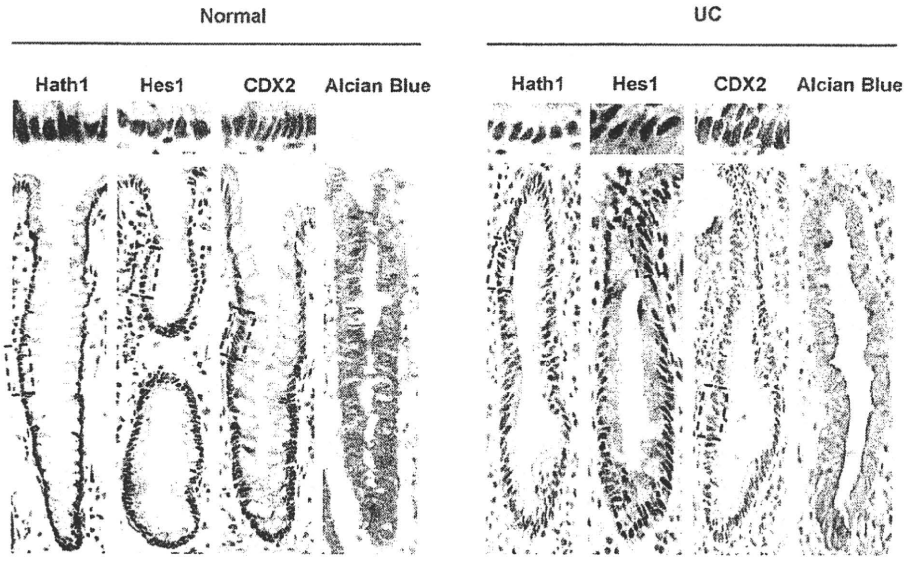

FIGURE 7. Immunohistochemistry of intestinal mucosa in UC. In normal colonic mucosa, Hath1 and CDX2 were expressed in most IEC. Hes1 was expressed in intestinal epithelial cells in the lower half of villi. In UC mucosa with goblet cell depletion, neither Hath1 nor CDX2 was expressed, whereas Hes1 was expressed up to the top of the villi. Upper column shows magnified view of the upper villus areas identified by dashed line in the lower column. Blue staining with Alcian blue represents goblet cells. The examination was performed by using the sections from three different individuals.

CDX2 is important to regulate *Hath1* gene expression, which is involved in goblet cell formation in UC. More detailed analysis of Hath1 expression at various stages of UC or other enteritis diseases associated with goblet cell depletion will lead us understand the regulation of Hath1 reduction under the inflammation state with various cytokines and inflammatory cells infiltration. Finally, elucidation of the mechanism of goblet cell depletion in UC will help us to develop novel therapies for strengthening the barrier function of colonic mucosa.

REFERENCES

1. Booth C, Brady G, Potten CS. Crowd control in the crypt. *Nat Med.* 2002;8:1360–1361.
2. El-Assal ON, Besner GE. HB-EGF enhances restitution after intestinal ischemia/reperfusion via PI3K/Akt and MEK/ERK1/2 activation. *Gastroenterology.* 2005;129:609–625.
3. Haramis AP, Begthel H, van den Born M, et al. De novo crypt formation and juvenile polyposis on BMP inhibition in mouse intestine. *Science.* 2004;303:1684–1686.
4. Clevers H. Wnt/beta-catenin signaling in development and disease. *Cell.* 2006;127:469–480.
5. Fre S, Huyghe M, Mourikis P, et al. Notch signals control the fate of immature progenitor cells in the intestine. *Nature.* 2005;435:964–968.
6. Oshima S, Nakamura T, Namiki S, et al. Interferon regulatory factor 1 (IRF-1) and IRF-2 distinctively up-regulate gene expression and production of interleukin-7 in human intestinal epithelial cells. *Mol Cell Biol.* 2004;24:6298–6310.
7. Crosnier C, Stamataki D, Lewis J. Organizing cell renewal in the intestine: stem cells, signals and combinatorial control. *Nat Rev Genet.* 2006;7:349–359.
8. Okamoto R, Tsuchiya K, Nemoto Y, et al. Requirement of Notch activation during regeneration of the intestinal epithelia. *Am J Physiol Gastrointest Liver Physiol.* 2009;296:G23–35.
9. Yang Q, Bermingham N, Finegold M, et al. Requirement of Math1 for secretory cell lineage commitment in the mouse intestine. *Science.* 2001;294:2155–2158.
10. Tsuchiya K, Nakamura T, Okamoto R, et al. Reciprocal targeting of Hath1 and beta-catenin by Wnt glycogen synthase kinase 3beta in human colon cancer. *Gastroenterology.* 2007;132:208–220.
11. Helms A, Abney A, Ben-Arie N, et al. Autoregulation and multiple enhancers control Math1 expression in the developing nervous system. *Development.* 2000;127:1185–1196.
12. Ebert PJ, Timmer JR, Nakada Y, et al. Zic1 represses Math1 expression via interactions with the Math1 enhancer and modulation of Math1 autoregulation. *Development.* 2003;130:1949–1959.
13. Murata K, Hattori M, Hirai N, et al. Hes1 directly controls cell proliferation through the transcriptional repression of p27Kip1. *Mol Cell Biol.* 2005;25:4262–4271.
14. Katz JP, Perreault N, Goldstein BG, et al. The zinc-finger transcription factor Klf4 is required for terminal differentiation of goblet cells in the colon. *Development.* 2002;129:2619–2628.
15. Jensen J, Pedersen EE, Galante P, et al. Control of endodermal endocrine development by Hes-1. *Nat Genet.* 2000;24:36–44.
16. Zheng H, Pritchard D, Yang X, et al. KLF4 gene expression is inhibited by the notch signaling pathway that controls goblet cell differentiation in mouse gastrointestinal tract. *Am J Physiol Gastrointest Liver Physiol.* 2009;296:G490–498.
17. Briggs KJ, Corcoran-Schwartz IM, Zhang W, et al. Cooperation between the Hic1 and Ptch1 tumor suppressors in medulloblastoma. *Genes Dev.* 2008;22:770–785.
18. Murata K, Hattori M, Hirai N, et al. Hes1 directly controls cell proliferation through the transcriptional repression of p27Kip1. *Mol Cell Biol.* 2005;25:4262–4271.
19. Mutoh H, Sakamoto H, Hayakawa H, et al. The intestine-specific homeobox gene Cdx2 induces expression of the basic helix-loop-helix transcription factor Math1. *Differentiation.* 2006;74:313–321.
20. Katoh M. Notch signaling in gastrointestinal tract (review). *Int J Oncol.* 2007;30:247–251.
21. Kageyama R, Ohtsuka T, Kobayashi T. The Hes gene family: repressors and oscillators that orchestrate embryogenesis. *Development.* 2007;134:1243–1251.

22. Monastirioti M, Giagtzoglou N, Koumbanakis K, et al. Drosophila Hey is a target of Notch in asymmetric divisions during embryonic and larval neurogenesis. *Development*. 2010;137:191–201.
23. Mukhopadhyay A, Jarrett J, Chlon T, et al. HeyL regulates the number of TrkC neurons in dorsal root ganglia. *Dev Biol*. 2009;334:142–151.
24. Chen H, Thiagalingam A, Chopra H, et al. Conservation of the Drosophila lateral inhibition pathway in human lung cancer: a hairy-related protein (HES-1) directly represses achaete-scute homolog-1 expression. *Proc Natl Acad Sci U S A*. 1997;94:5355–5360.
25. Gersemann M, Becker S, Kubler I, et al. Differences in goblet cell differentiation between Crohn's disease and ulcerative colitis. *Differentiation*. 2009;77:84–94.
26. Shroyer NF, Helmrath MA, Wang VYC, et al. Intestine-specific ablation of mouse atonal homolog 1 (Math1) reveals a role in cellular homeostasis. *Gastroenterology*. 2007;132:2478–2488.
27. Dahan S, Roda G, Pinn D, et al. Epithelial: lamina propria lymphocyte interactions promote epithelial cell differentiation. *Gastroenterology*. 2008;134:192–203.
28. Colleypriest B, Palmer R, Ward S, et al. Cdx genes, inflammation and the pathogenesis of Barrett's metaplasia. *Trends Mol Med*. 2009;15: 313–322.
29. Eda A, Osawa H, Yanaka I, et al. Expression of homeobox gene CDX2 precedes that of CDX1 during the progression of intestinal metaplasia. *J Gastroenterol*. 2002;37:94–100.
30. Zheng J, Sun X, Wang W, et al. Hypoxia-inducible factor-1alpha modulates the down-regulation of the homeodomain protein CDX2 in colorectal cancer. *Oncol Rep*. 2010;24:97–104.
31. Giatromanolaki A, Sivridis E, Maltezos E, et al. Hypoxia inducible factor 1alpha and 2alpha overexpression in inflammatory bowel disease. *J Clin Pathol*. 2003;56:209–213.

J Gastroenterol
DOI 10.1007/s00535-010-0346-x

ORIGINAL ARTICLE—ALIMENTARY TRACT

Longitudinal cell formation in the entire human small intestine is correlated with the localization of Hath1 and Klf4

Michiko Iwasaki · Kiichiro Tsuchiya · Ryuichi Okamoto · Xiu Zheng · Yoshihito Kano · Eiko Okamoto · Eriko Okada · Akihiro Araki · Shinji Suzuki · Naoya Sakamoto · Keisuke Kitagaki · Takumi Akashi · Yoshinobu Eishi · Tetsuya Nakamura · Mamoru Watanabe

Received: 26 July 2010 / Accepted: 18 October 2010

Abstract
Background Double balloon endoscopy (DBE) enables the observation and collection of viable specimens from the entire intestine, thereby allowing more detailed investigation of how the structure and function of the human small intestine are regulated. The present study aimed to elucidate the regulation of cell formation in the human small intestine using biopsy specimens collected from an entire individual small intestine by DBE.

Methods The expression and the localization of representative genes for the differentiation program were analyzed in the entire small intestine of 10 patients. The functional correlation between Hath1 and Klf4 was analyzed in an intestinal cell line by using a Tet-On system.

Results In longitudinal cell formation in the small intestine, it was shown that goblet cells, but not Paneth cells, increased toward the ileum in each individual small intestine. Immunohistochemistry showed that Hath1-expressing cells migrated from the base of the crypt to the top of the villi in the terminal ileum, while Klf4-expressing cells migrated from the top of the villus, resulting in the colocalization of Hath1 and Klf4 in the terminal ileum. Coexpression of Hath1 and Klf4 upregulated the expression of phenotypic genes for goblet cells following the downregulation of those for Paneth cells.

Conclusions Using mapping biopsy by DBE, we have demonstrated, for the first time, the molecular basis of the villus structure in the entire human small intestine in vivo. The present study showed that longitudinal cell formation was regulated by the colocalization of Hath1 and Klf4 that converted Paneth cell differentiation into goblet cell differentiation.

Keywords Double balloon endoscopy · Goblet cells · Paneth cells · Hath1 · Atoh1

M. Iwasaki and K. Tsuchiya contributed equally to this work.

Electronic supplementary material The online version of this article (doi:10.1007/s00535-010-0346-x) contains supplementary material, which is available to authorized users.

M. Iwasaki · K. Tsuchiya · R. Okamoto · X. Zheng · Y. Kano · E. Okamoto · E. Okada · A. Araki · S. Suzuki · N. Sakamoto · T. Nakamura · M. Watanabe (✉)
Department of Gastroenterology and Hepatology, Graduate School, Tokyo Medical and Dental University, 1-5-45, Yushima, Bunkyo-ku, Tokyo 113-8519, Japan
e-mail: mamoru.gast@tmd.ac.jp

R. Okamoto · T. Nakamura
Department of Advanced Therapeutics in Gastrointestinal Diseases, Graduate School, Tokyo Medical and Dental University, Tokyo, Japan

N. Sakamoto
Department for Hepatitis Control, Tokyo Medical and Dental University, Tokyo, Japan

E. Okada · A. Araki
Department of Endoscopic Diagnosis and Therapy, Tokyo Medical and Dental University, Tokyo, Japan

K. Kitagaki · T. Akashi · Y. Eishi
Department of Pathology, Graduate School, Tokyo Medical and Dental University, Tokyo, Japan

Introduction

The six-meter length of the human small intestine consisting of the jejunum and ileum had long been considered a "dark continent" because of the lack of devices to observe its whole length easily. Recently, however, powerful tools have been developed to visualize the whole

Published online: 03 December 2010

human intestinal tract, such as capsule endoscopy (CE) [1, 2] and double balloon endoscopy (DBE) [3–5]. These have revealed an unexpectedly large number of diseases of the small intestine, such as cancers, malignant lymphomas, ulcers, and vascular lesions [6, 7]. At the same time, a number of ulcerous and erosive lesions found by histopathological examination of biopsy specimens have been observed as unknown diseases with nonspecific inflammation [8]. Therefore, elucidation of pathobiological regulation in the human small intestine is essential to resolve the difficulty of diagnosing the various lesions in the small intestine.

Despite the multiple roles of the small intestine in homeostasis, such as digestion, absorption, immune regulation, hormone secretion, peristaltic movement, and the regeneration of intestinal epithelial cells (IECs) [9–12], the overall function of the entire small intestine has never been considered. Although the horizontal structure of the small intestine has been elucidated as showing axial regulation from crypt base to villus top under the control of various signal transduction pathways, such as Wnt, Notch, and bone morphogenetic protein (BMP) [13–16], the regulation of its longitudinal structure remains to be elucidated, especially in humans. An understanding of the molecular basis of the structure of the human intestine has been thought to be indispensable for elucidating the pathology of human intestinal disease. One of the most important genes for the formation of IECs is that for the basic helix-loop-helix (bHLH) transcription factor, Atoh1, and its human homolog, Hath1, which is essential for cellular differentiation toward secretory lineages in the small and large intestine [17]. According to our recent studies, failure of the differentiation system in the human colon is caused by the deregulation of crucial genes for the construction of IECs with aberrant cell signaling induced by the pathology of intestinal diseases, such as colon cancer and ulcerative colitis [18, 19].

It has been suggested that regional functions of the small intestine might be different, with rigid regulation for the immediate situation in each region from the proximal side to the distal side. However, the regional roles of IECs have been poorly investigated, except for their part in nutritional absorption and hormone secretion [9, 20]. Moreover, it remains unknown how the ratio of the four lineages of IECs—goblet cells, enteroendocrine cells, Paneth cells, and absorptive enterocytes—is regulated to fit to regional function in the human small intestine. Hitherto, analyses of regional function in the human small intestine have employed specimens originating from operative tissues of different individuals [21, 22]. Accordingly, those results are not precisely comparable because of individual differences, although it has been widely considered that the number of goblet cells and Paneth cells increases toward the terminal ileum.

Although cellular differentiation into goblet cells is regulated by Atoh1 and a zinc-finger type transcriptional factor, Kruppel-like factor 4 (Klf4) [17, 23], the mechanism by which goblet cells increase in number toward the terminal ileum has not yet been elucidated.

In this study, we performed a mapping biopsy of the entire human small intestine using DBE to elucidate the regional regulation of cell formation in the villi. We found an increase in the number of goblet cells, but not Paneth cells, toward the terminal ileum. The colocalization of Hath1 and Klf4 proteins changed cellular differentiation to Paneth cells to differentiation to goblet cells, regulating the longitudinal differentiation of cells in the human small intestine.

Materials and methods

Human small intestinal tissue

Human tissue specimens were obtained from patients with an indication to undergo DBE at Tokyo Medical and Dental University Hospital because of obscure gastrointestinal bleeding. To analyze the structure of the normal small intestine, we selected biopsy specimens from 10 patients who showed no abnormality in the small intestine by subsequent DBE. Patients with abnormal findings in the small intestine by DBE and those who were taking medication that might injure the small intestinal mucosa were excluded. To measure villus size, tissue specimens from 20 patients with no abnormality in the small intestine by DBE were used. Written informed consent was obtained from each patient, and the experiments were approved by the Tokyo Medical and Dental University Hospital Ethics Committee for Human Subjects.

The proximal two-fifths of the small intestine was observed via the oral insertion route, and biopsy specimens were taken from two locations at approximately equal intervals. On another day, the distal three-fifths of the small intestine was observed via the anal insertion route, and biopsy specimens were taken from three locations at approximately equal intervals. Biopsy intervals were confirmed from the position of the endoscope tip visualized by X-ray and from the insertion length of the endoscope calculated by addition of the insertion lengths in each operation. Three biopsy specimens were taken from each of the five locations in each patient to generate RNA, paraffin sections, and frozen sections, respectively. Each biopsy specimen was numbered 1–5 from the proximal side.

Quantitative real-time polymerase chain reaction (PCR)

Total RNA was isolated using TRIzol reagent (Invitrogen; Carlsbad, CA, USA). Aliquots of 1 μg of total RNA were used for reverse transcription (Qiagen; Valencia, CA, USA). Quantitative PCRs were carried out using a Light-Cycler system (Roche Diagnostics; Mannheim, Germany). The primer sequences are summarized in supplementary Table S1. In the analysis of small intestine biopsy specimens, the expression of the most proximal specimen was taken as 1 in order to compensate for individual differences.

Histology and immunohistochemistry

Histological analysis of human small intestines was performed by using hematoxylin and eosin (H&E)-stained slices or periodic acid-Schiff (PAS)-stained slices generated from paraffin sections. The height and width of the villus mucosa and the depth of crypts were measured with a Micro Analyzer (Japan Poladigital; Tokyo, Japan). Three villi and crypts per slide of each region in 10 patients were measured.

Immunohistochemical findings from human small intestines were assessed by using frozen sections. Hath1 antibody was originally generated as previously described [18]. Hes1 antibody was the same as that used in a previous study [19]. The other antibodies used were anti-human chromogranin A (CgA) (DAKO; Glostrup, Denmark), anti-human Klf4 (H-180; Santa Cruz Biotechnology; Santa Cruz, CA, USA), and anti-human TFF3 (ab57752; Abcam; Cambridge, UK). The standard avidin-biotin-peroxidase (ABC) method (Vectastain; Vector Laboratories; Burlingame, CA, USA) was used, and staining was developed by the addition of diaminobenzidine (Vector Laboratories).

Goblet cells were counted per 300 epithelial cells. Paneth cells were counted per crypt. These two types of cells were counted on H&E-stained slices. Endocrine cells were counted as CgA-positive cells per 300 epithelial cells on CgA-immunostained slices. The number of absorptive cells was calculated by subtracting the goblet cell and CgA-positive cell numbers from the total number.

Cell culture

Human colon cancer-derived LS174T cells were grown in minimum essential medium (Gibco; Billings, MT, USA) supplemented with 10% fetal bovine serum and 1% penicillin–streptomycin. The cell cultures and plasmid DNA transfections were performed as previously described [24]. A cell line expressing Klf4 (Tet-On Klf4 cells) under the control of doxycycline (DOX, 100 ng/ml; Clontech; Mountain View, CA, USA) was generated as previously described [25].

Plasmids

Hath1-lentivirus vector was generated by inserting the PCR-amplified Hath1 gene into pLenti6.4 (Invitrogen). Hath1-lentivirus was generated according to the manufacturer's protocols.

Tetracycline-dependent expression of Klf4 was achieved by cloning the gene encoding the open reading frame of the human Klf4 into the pcDNA4/TO/myc-his vector (Invitrogen). All constructs were confirmed by DNA sequencing.

Statistical analyses

In the quantitative real-time PCR analysis of small-intestine biopsy specimens, groups of data were compared using the Mann–Whitney U-test. P values of less than 0.05 were considered statistically significant.

Other data were statistically analyzed with paired Student's t-tests. P values of less than 0.05 were considered statistically significant.

Results

The villus height, width, and crypt depth in an entire small intestine were the same in all longitudinal regions

While regional differences between the jejunum and the ileum have been found anatomically, distinct differences between them in villus structure have not been suggested. Moreover, the precise mechanism for the formation of a regional villus structure has not been examined in a full-length small intestine in an "alive environment". We therefore performed mapping biopsy of the full-length small intestine in 10 people who had an indication for DBE. We determined the positions for biopsy with the assistance of X-ray images and the insertion length of the endoscope in order to take five biopsy specimens at equal intervals from the ligament of Treitz to Bauhin's valve. The resulting regions were numbered 1–5 from the proximal side (Fig. 1a). The endoscopic findings of the whole small intestine were normal, and neither inflammation nor erosion was found by pathological examinations of biopsy samples (Fig. 1b).

We first analyzed the villus size, dividing it into height, width, and crypt depth, throughout the small intestine. Unexpectedly, the villus size in each of 20 people was almost the same in any region of the small intestine (Fig. 1c). Previous reports showed that the villi became

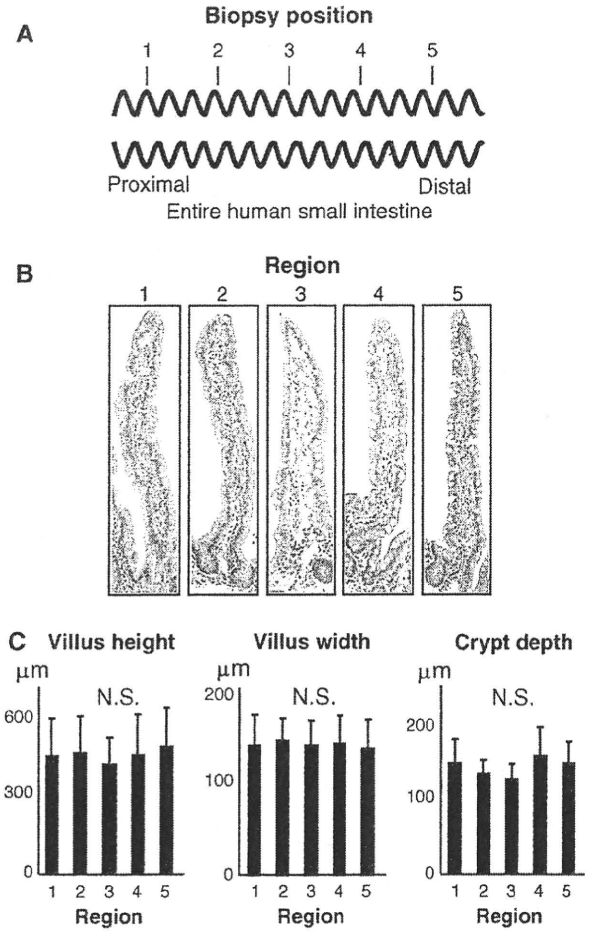

Fig. 1 Structure of villi and crypts throughout the entire human small intestine. **a** Schematic representation of the position for mapping biopsy by double balloon endoscopy (DBE). **b** H&E-stained sections of biopsy specimens (×10). Specimens are numbered 1–5 from proximal to distal regions. Fundamental structures of villi and crypts do not change throughout the entire human small intestine. Paneth cells are observed as acidophilic cells at the base of crypts. **c** Villus height, villus width, and crypt depth. The size of villi and crypts was constant from proximal to distal regions (differences not significant, P [0.05, n = 20). N.S. Not significant

shorter and wider toward the terminal ileum in rats [26]. In humans, in studies using operative or anatomical tissues, it has also been thought that villus length was greater at the proximal jejunum than at the terminal ileum; however, the villus size of the entire small intestine of the same person has never been analyzed in vivo.

Goblet cells increased toward the terminal ileum, while Paneth cells were maintained

We next assessed the longitudinal change of cell formation in the villi of individual human small intestines by counting each of four types of IECs in each region. PAS staining showed a phased increase of goblet cells toward the terminal ileum (Fig. 2a, d), while surprisingly, the number of Paneth cells per crypt was unchanged, which contradicts the widely accepted hypothesis that Paneth cells are increased toward the terminal ileum (Fig. 2b, d). CgA-positive cells were counted as endocrine cells (Fig. 2c, d), and cells other than the foregoing three types were counted as absorptive cells, and their numbers decreased toward the terminal ileum (Fig. 2d).

We also assessed the regional expression of representative genes for each type of cell to confirm whether gene expression parallels cell formation in each region of the small intestine. Quantitative real-time PCR revealed considerable individual differences between the 10 people in gene expression at the same position in the small intestine (Fig. 2e). To compensate for this, the gene expression in each region was expressed relative to that in region 1 in the jejunum, which was taken as unity. MUC2 gene expression gradually increased in the same way as the cell formation. In regions 4 and 5, MUC2 expression was significantly increased compared with that in region 1, while lactase gene expression was significantly decreased compared with that in region 1.

Interestingly, the expression of HD5 was almost constant throughout the small intestine, consistent with Paneth cell formation, and differed from expectations that antimicrobial peptides would be induced by the increase of enterobacteria in the terminal ileum. The quantities of intestinal epithelial cells included in each biopsy specimen were found to be constant by cytokeratin 19 (CK19) quantification in each region (Supplemental Fig. 1).

The increase of Hath1 gene expression at the terminal ileum is independent of the Notch signal

To clarify how the transition of cell formation in each region is regulated, we examined the gene expression of Hath1 and Hes1, because the Notch signal determines the fate of IECs, especially the differences between absorptive cells and secretory cells, through the expression of the Hes1 and Hath1 genes, respectively, as we and others have previously described [14, 19]. The Hath1 genes were upregulated toward the terminal ileum, while Hes1 gene expression was unchanged (Fig. 3a). We also analyzed the localization of Hath1 in the villi in each region. In region 1, Hath1-positive cells were found only at the crypt base. However, toward the ileum, Hath1 expression gradually ascended to the villi. Finally, in region 5, Hath1-positive cells were found throughout the whole villus (Fig. 3b). In contrast, Hes1-positive cells were found in the crypt base in all regions of the human small intestine (Fig. 3b). We also counted the number of each type of protein-positive cell in each region. In the crypts, Hath1- and Hes1-positive cells